



HAL
open science

Autophosphorylation-independent and -dependent functions of focal adhesion kinase during development.

Jean-Marc Corsi, Christophe Houbron, Pierre Billuart, Isabelle Brunet, Karine Bouvrée, Anne Eichmann, Jean-Antoine Girault, Hervé Enslin

► To cite this version:

Jean-Marc Corsi, Christophe Houbron, Pierre Billuart, Isabelle Brunet, Karine Bouvrée, et al.. Autophosphorylation-independent and -dependent functions of focal adhesion kinase during development.: FAK without phosphorylation. *Journal of Biological Chemistry*, 2009, 284 (50), pp.34769-76. 10.1074/jbc.M109.067280 . inserm-00432666

HAL Id: inserm-00432666

<https://inserm.hal.science/inserm-00432666>

Submitted on 23 Sep 2010

HAL is a multi-disciplinary open access archive for the deposit and dissemination of scientific research documents, whether they are published or not. The documents may come from teaching and research institutions in France or abroad, or from public or private research centers.

L'archive ouverte pluridisciplinaire **HAL**, est destinée au dépôt et à la diffusion de documents scientifiques de niveau recherche, publiés ou non, émanant des établissements d'enseignement et de recherche français ou étrangers, des laboratoires publics ou privés.

Autophosphorylation-independent and dependent functions of Focal Adhesion Kinase during development

Jean-Marc Corsi ^{*,†,§}, Christophe Houbron ^{‡,§§}, Pierre Billuart ^{‡,§§}, Isabelle Brunet ^{‡‡}, Karine Bouvrée ^{‡‡}, Anne Eichmann ^{‡‡}, Jean-Antoine Girault ^{*,†,§} and Hervé Enslen ^{*,†,§,1}

^{*}Inserm U839, 17 rue du Fer-à-Moulin, 75005 Paris, [†]UPMC-Paris 6, Paris, 75005 Paris, [§]Institut du Fer-à-Moulin, 75005 Paris, [‡]Inserm U567 Paris and ^{§§} Institut Cochin, Université Paris Descartes and CNRS, UMR8104, Paris 75014, ^{‡‡} Collège de France, Inserm U833, 75005 Paris, France.

(1) Correspondence: Inserm U567, Institut Cochin, Bat. G. Roussy (5eme étage), 27 rue du Faubourg St-Jacques, 75014 Paris France. Tel: +33-40-51-65-54, Fax: +33-40-51-65-50. Email: herve.enslen@inserm.fr

Focal adhesion kinase (FAK) regulates numerous cellular functions and is critical for processes ranging from embryo development to cancer progression. Although autophosphorylation on Tyr-397 appears required for FAK functions *in vitro*, its role *in vivo* has not been established. We addressed this question using a mutant mouse (*fak^Δ*) deleted of exon 15, which encodes Tyr-397. The resulting mutant protein FAK Δ is an active kinase expressed at normal levels. Our results demonstrate that the requirement for FAK autophosphorylation varies during development. FAK $\Delta\Delta$ embryos developed normally up to E12.5, contrasting with the lethality at E8.5 of FAK-null embryos. Thus, autophosphorylation on Tyr-397 is not required for FAK to achieve its functions until late mid-gestation. However, FAK $\Delta\Delta$ embryos displayed hemorrhages, oedema, delayed artery formation, vascular remodelling defects, multiple organs abnormalities, and overall developmental retardation at E13.5-14.5, and died thereafter demonstrating that FAK autophosphorylation is also necessary for normal development. Fibroblasts derived from mutant embryos had a normal stellate morphology and expression of focal adhesion proteins, Src family members, p53 and Pyk2. In contrast, in FAK $\Delta\Delta$ fibroblasts and endothelial cells spreading and lamellipodia formation were altered with an increased size and number of focal adhesions, enriched in FAK Δ . FAK mutation also decreased fibroblasts proliferation. These results show that the physiological functions of FAK *in vivo* are achieved through both autophosphorylation-independent and autophosphorylation-dependent mechanisms.

Focal adhesion kinase (FAK) is a non-receptor tyrosine kinase critical for processes ranging from

embryo development (1) to cancer invasiveness and metastasis (2). FAK activation following integrin engagement or stimulation of a variety of transmembrane receptors, triggers its phosphorylation on tyrosine and the formation of multimolecular signaling complexes (3). FAK is enriched in focal adhesions, controlling their turnover and consequently adhesion-related processes such as spreading, migration, survival and proliferation (1).

The important physiological role of FAK is demonstrated by the lethality of its null mutation at embryonic day (E) 8.5 (4, 5). Further studies using conditional deletion showed that FAK regulates the development of the nervous system (6-9), morphogenesis of the vascular network (5, 10, 11), and cardiac development (12-15). These reports clearly established that FAK is necessary for essential processes *in vivo*.

In vitro studies have shown that, following its recruitment to focal adhesions, FAK autophosphorylation on Tyr-397 creates a high-affinity binding site for multiple signaling proteins including the Src family kinases (SFKs) (3). Following their binding to phospho-Tyr-397 and activation, SFKs phosphorylate other FAK residues inducing its complete activation, its interaction with other signaling proteins and the stimulation of downstream signalling cascades (16). The FAK-SFK complexes also regulate cytoskeleton rearrangement and downstream signaling pathways by phosphorylating partner proteins such as p130Cas and paxillin (17, 18). Thus FAK autophosphorylation on Tyr-397 appears to be critical for both FAK activation and scaffolding function *in vitro*, triggering the assembly of multimolecular complexes responsible for its cellular effects. Interestingly recent results showed that pharmacological inhibition of FAK activity and autophosphorylation did not block tumor cells proliferation and apoptosis *in vitro* (19), suggesting that FAK may also have autophosphorylation-

FAK without autophosphorylation

independent functions (20). Therefore it is particularly important to determine the role of Tyr-397 in FAK functions *in vivo*.

Here we addressed this question using a mutant mouse deleted of FAK exon 15, which encodes 19 amino acids including Tyr-397 (21). Our results show that the requirement for FAK autophosphorylation varies during development and demonstrate that the physiological functions of FAK *in vivo* are achieved through both autophosphorylation-independent and autophosphorylation-dependent mechanisms.

EXPERIMENTAL PROCEDURES

Generation of *FAK^{Δ/Δ}* mice-*FAK^{Δ/Δ}* mice were generated (see also Supplemental Fig.1) in the course of experiments aiming at testing the role of FAK alternatively spliced exons (22). A DNA fragment containing exons 13-18 from the mouse *Ptk2* gene was isolated from a SV129 genomic library (RPCI21MPAC, clone identification RPCIP711H19216Q2; RZPD, Berlin, Germany) and subcloned to construct the targeting vector (Supplemental Fig.1A). Embryonic stem (ES) cells isolated from male SV129 were electroporated with the targeting vector. Transfected cells were selected with hygromycin, 24 hours later and tested by PCR and Southern blotting (Supplemental Fig. 1A and B). For the present study we selected a clone which exhibited the homologous recombination event and an additional spontaneous deletion of a 307 bp genomic fragment including exon 15 (nt 34393031 to 34393338 of FAK gene sequence NT_039621.7). This mutant allele of *FAK* gene was named *FAK^Δ*. C57BL/6 blastocysts were injected with *FAK^{Δ/+}* ES cell and transferred to pseudo-pregnant mice. Male chimeric mice carrying the *FAK^Δ* allele were mated to C57BL/6 female mice and offspring were genotyped based on their coat colour.

Animal Care-*FAK^{+/-}* mice were produced and maintained in the *Fer-à-Moulin* Institute animal house in stable conditions of temperature (22°C) and humidity (60%) with a constant cycle of 12h light and 12h dark and free access to food and water. All experiments were in accordance with the guidelines of the French Agriculture and Forestry Ministry for handling animals (decree 87849, license A 75-05-22).

Genotyping by PCR-Mice and embryos were genotyped by PCR analysis (details in Supplemental Fig. 4) using DNA extracted from tail biopsies.

Antibodies-Sources: pY-397-FAK, pY-418-Src and pY421-cortactin: Biosource Inc; pY-118-paxillin, pY-410-p130Cas, pY-576/577-FAK and pY-925-FAK: Cell Signaling Inc; FAK (clone 4.47) and cortactin: Upstate Biotechnology Inc; Fyn (FYN3), Src (SRC2), FAK (C-20) and GAPDH: Santa-Cruz Biotechnology Inc; rat PECAM-1 monoclonal CD31 (clone MEC13.3), CD102, p130Cas, paxillin: Beckton Dickinson Biosciences; biotinylated TuJ1: R&D systems; smooth muscle α -actin-FITC (mouse clone 1A4) and vinculin: Sigma-Aldrich Inc. Pyk2 rabbit antibody was produced in house. Rhodamin-conjugated phalloidin and all secondary antibodies (AlexaFluor) were from Molecular Probes, Invitrogen Inc, and Jackson Immune Research Laboratory.

Whole mount staining-Embryos were fixed in 4% paraformaldehyde in PBS. After dehydration in a series of methanol, they were treated with 1% H₂O₂, rehydrated from methanol to PBS, and blocked in 4% (w/v) bovine serum albumin- 0.1% (v/v) Triton X-100. They were then incubated with anti-PECAM-1 (1:500) in 4% BSA 0.1% Triton X-100 in PBS at 4°C overnight followed by peroxidase-conjugated secondary antibody. The reaction was developed in 0.03% 3-3'-diaminobenzidine with H₂O₂. For the whole-mount skin immunostaining, skins were removed after embryo fixation, permeabilized for 2 hours (0,2% triton X100) and blocked (Roche, ref 11096176001) for 2 hours prior to incubation with antibodies against PECAM-1 and biotinylated TuJ1 (1:200 dilution) in 0.1% triton + 1% BSA+ 1% Goat serum overnight at 4°C. After washes for 4 hours, skins were incubated with secondary antibody (AlexaFluor 555 goat anti-rat) and monoclonal anti smooth muscle α -actin-FITC in blocking solution for 2 hours. Acquisitions were performed with a confocal microscope (Leica, SP5, 10x magnification).

Tissue extraction and preparation for immunoblotting-Tissues and organs from embryos or adult mice were frozen immediately after dissection and sonicated later in 100°C, 1% (w/v) SDS (1%) containing NaVO₄ (1 mM), placed in a 100°C heating block for 3 min and processed as described in the immunoblotting section.

Cell culture-COS7 cells were grown and transfected with Lipofectamin 2000 (Invitrogen) as previously described (23). For the primary fibroblasts, four *FAK^{+/+}* and 3 *FAK^{Δ/Δ}* independent mouse embryonic fibroblasts (MEF) populations were prepared from 7 littermates E12.5 embryos of 2 different litters obtained from heterozygous

FAK without autophosphorylation

crossings and cultured as described (24). All experiments were performed between passage 1 and 3. The 7 MEF populations were tested separately in each experiment. Primary endothelial cells (EC) were isolated from $FAK^{+/+}$ and $FAK^{\Delta/\Delta}$ E12.5 and E13.5 embryos using magnetic beads (Dynabead M-450; Dynal Corp.) and rat anti-mouse PECAM-1 (CD31) (5). For the fibronectin replating experiments, MEF or EC were prepared as described (25) before being plated on tissue culture dishes or glass coverslips precoated with polylysine (50 $\mu\text{g/ml}$) or fibronectin (10 $\mu\text{g/ml}$) and processed for immunoblotting or immunofluorescence at the indicated times.

Immunoblotting-After the appropriate treatment, cells were rinsed, frozen on dry ice, lysed with boiling SDS (1%) containing NaVO_4 (1 mM), sonicated and boiled for 3 min. Protein concentration was determined with the BCA assay (Pierce) and 50 to 100 μg of protein were analyzed by SDS-PAGE. Quantification of immunoblots was performed with Odyssey Li-Cor. Data were normalized to the mean value of untreated controls in the same autoradiograms.

Immunofluorescence-Cells were fixed for 15 minutes in 4% (w/v) PFA and permeabilized with TritonX100 0.05% for 5 min. After blocking and incubation with primary antibody overnight, cells were incubated with Alexa-488- or Cy3-coupled secondary antibodies or rhodamin-conjugated phalloidin (1/400) for 1 hour and mounted in Vectashield with DAPI. Acquisition of the images was performed on a Leica DM600B equipped with a numerical camera CCD Micromax (Princeton Instrument) at 20x (N.A. 0.7, PL APO) or 40x (N.A. 1.25, oil, PL APO) using Metamorph software. In experiments with EC, only cells positive for CD31 or CD102 were selected for analysis of immunofluorescence with antibodies recognizing other proteins.

Proliferation studies-MEFs were plated separately in triplicate at 7500 cells/well in 24-well plates. The growing medium was changed every other day and cells were fixed everyday with cold methanol and kept at -20°C until the end of the experiment. At that time cells were stained with crystal violet staining and solubilized (24) and cell number was estimated with a spectrophotometer at 590 nm. Data points were the average of triplicates.

RESULTS AND DISCUSSION

Generation of $fak\Delta$ mice expressing an active but autophosphorylation-deficient mutant form of FAK-

Mutant mice ($fak\Delta$) were generated from ES cells in which FAK exon 15 (21) was deleted by homologous recombination (Supplemental Fig. 1, A and B). Analyses of tissues from heterozygous $FAK^{+/\Delta}$ mice by RT-PCR (data not shown) and western blotting (Supplemental Fig. 1C), confirmed that the deletion of exon 15 did not alter FAK mRNA open reading frame, resulting in the expression of the expected full length mutant protein FAK Δ deleted of the 19 residues (including Tyr-397) coded by exon 15 and located between the N-terminal four-point-one, ezrin, radixin, moesin (FERM) and kinase domains (21) (Fig. 1A). FAK Δ was expressed at the same levels as normal FAK encoded by the wild type allele (Supplemental Fig. 1C). As expected, FAK Δ was not detected by P-Tyr-397-specific antibodies in transfection experiments. Using a transphosphorylation assay in COS7 cells (23), we found that the basal kinase activity of FAK Δ , was moderately increased (Supplemental Fig. 2). Thus $fak\Delta$ mice constitute an interesting model to study the role of FAK autophosphorylation *in vivo*.

FAK Δ/Δ mice display multiple abnormalities after mid-gestation and lethality between E14.5 and E16.5-The intercrossing of $FAK^{+/\Delta}$ mice produced only 0.25% $FAK^{\Delta/\Delta}$ pups (Table 1) compared to the expected mendelian ratio of 25%. This result suggested that the dizygous expression of FAK Δ was lethal for the vast majority of $FAK^{\Delta/\Delta}$ embryos. To define the stage at which the $FAK^{\Delta/\Delta}$ embryos died and to compare their phenotype to $FAK^{+/+}$ embryos, dated embryos were collected during development and genotyped by PCR. At E11.5 and E12.5, living $FAK^{\Delta/\Delta}$ embryos were found at mendelian ratios (Table 1 and Fig. 1B). They were indistinguishable from their control littermates in morphology and development and showed normal vascularization by whole-mount anti-PECAM1 immunostaining (Supplemental Fig. 3A and data not shown). At E13.5, $FAK^{\Delta/\Delta}$ embryos were smaller than $FAK^{+/+}$ embryos and showed abnormal superficial vasculature, hemorrhagic liver, multiple body hemorrhages and oedemas (Fig. 1C), indicating that FAK autophosphorylation was required for normal development after E12.5. A decrease in the ratios of living $FAK^{\Delta/\Delta}$ embryos compared to wild type was observed between E13.5 and E15.5 and very few survived past E16.5 (Table 1 and Fig. 1B). $FAK^{\Delta/\Delta}$ embryos also showed alteration and retardation in heart, lung, liver and limbs development at E14.5 (Fig. 1C) and yolk sac

FAK without autophosphorylation

vascularization defects were observed at E15.5 (Supplemental Fig. 3B). Since vascular defects were observed in $FAK^{\Delta/\Delta}$ embryos from E13.5, we further investigated vascular development by performing skin whole-mount immunofluorescence from E14.5 embryos. Smooth muscle actin staining was visible on arteries formed in the skin of wild type embryos, whereas $FAK^{\Delta/\Delta}$ arteries only showed weak smooth muscle actin staining in the proximal part. In addition, there was a defect in the remodelling of the vascular plexus in $FAK^{\Delta/\Delta}$ embryos (Fig. 1D). These results demonstrate that the homozygous FAK mutation deleting the autophosphorylation site, resulted in vascular defects and developmental retardation apparent at E13.5, and embryonic lethality between E14.5 and E16.5. Although the stage of embryonic lethality caused by the early conditional deletion of FAK in endothelial cells remains controversial (5, 10), one study reported lethality between E13.5 and E14.5 with a phenotype very similar to what we observed in $FAK^{\Delta/\Delta}$ embryos (5). Thus, it is likely that vascular abnormalities were an important factor in embryonic lethality, although we cannot exclude that failure of other organs also played a role.

The mid-gestation lethality of $FAK^{\Delta/\Delta}$ embryos contrasted with the early developmental lethality at E8.5 reported in FAK-null embryos (4, 26) even in the same genetic background as $fak\Delta$ mice (5). Comparison of the survival of $FAK^{\Delta/\Delta}$ and $FAK^{-/-}$ embryos during development confirmed that the absence of FAK led to an earlier developmental lethality than the absence of FAK autophosphorylation (Fig. 1B). Thus, FAK requirement for normal development is independent of its autophosphorylation until E13.5. Moreover, we observed rare (0.25%) verified $FAK^{\Delta/\Delta}$ mice, which survived to adulthood and were fertile (Table 1 and Supplemental Fig. 4) whereas no FAK-null adult mice have been reported (4, 5, 26). This observation demonstrates that the absence of FAK autophosphorylation can be compensated in very rare cases *in vivo*.

FAK^{Δ/Δ} mutation has minor effect on the levels of associated proteins-Next we monitored the expression of FAK Δ and FAK-associated proteins in mutant embryos. FAK Δ protein was expressed at the same level as FAK in $FAK^{+/Δ}$ embryos, or in $FAK^{\Delta/\Delta}$ embryos compared to $FAK^{+/+}$ embryos at every developmental stage tested, but, as expected, only FAK was phosphorylated on Tyr-397 (Fig. 2A and data not shown). Since the cytoskeleton

rearrangements and downstream signaling pathways regulated by FAK are mediated by its interaction with SFKs and focal adhesions proteins such as paxillin and p130Cas (17, 18), we also monitored their expression. We found in E14.5 mutant embryos, a moderate increase in the expression of paxillin and p130Cas, as well as cortactin (Fig. 2A) which facilitates cortical actin polymerization (27). In contrast, vinculin, another focal adhesion protein anchoring F-actin to the membrane, and Src and Fyn were expressed at the same levels in $FAK^{+/+}$ and $FAK^{\Delta/\Delta}$ embryos (Fig. 2A). The FAK-related tyrosine kinase Pyk2 was barely detectable in both $FAK^{+/+}$ and $FAK^{\Delta/\Delta}$ embryos and no increase was observed in mutant mice at any developmental stage tested (data not shown). Interestingly, a very strong increased expression of Pyk2 and paxillin has been reported in some FAK-null tissues or cell types (11, 20, 25, 28, 29) and Pyk2 overexpression can functionally compensate FAK absence (11, 25, 28, 29) and/or have unrelated deleterious consequences (28). Based on these results it has been proposed that FAK maintains a low level of Pyk2 expression in normal conditions in some tissues or cell types (11, 28). The lack of Pyk2 upregulation in $FAK^{\Delta/\Delta}$ embryos, suggests that FAK autophosphorylation is not required to maintain a low level of Pyk2 expression during development *in vivo*. Our results also support the hypothesis that Pyk2 overexpression might contribute to the severity of FAK-null mutation (20, 28).

In order to characterize the cellular consequences of the mutation on the regulation of associated proteins, we studied primary mouse embryonic fibroblasts (MEFs) from E12.5 $FAK^{+/+}$ and $FAK^{\Delta/\Delta}$ embryos. Western blotting experiments showed that FAK Δ was expressed at the same levels in $FAK^{\Delta/\Delta}$ MEFs as FAK in $FAK^{+/+}$ MEFs (Fig. 2B). Only a moderate increase (<2-fold) in the level of Pyk2 was observed in these cells compared to $FAK^{+/+}$ MEFs (Fig. 2B). This result contrasted with the strong overexpression of Pyk2 that we observed in $FAK^{-/-}$ fibroblasts (~10 fold, data not shown) and that had also been previously reported (25, 28, 29). The levels of vinculin, p130Cas, paxillin, cortactin, Fyn and Src, were not changed by the $fak^{\Delta/\Delta}$ mutation in MEFs (Fig. 2B). Finally, similarly to $FAK^{+/+}$ MEFs, no p53 was detected in $FAK^{\Delta/\Delta}$ MEFs (Fig. 2C) in contrast to its strong expression in primary $FAK^{-/-}$ fibroblasts (20). Thus, $FAK^{\Delta/\Delta}$ MEFs are an interesting model to study the effects of the FAK mutant lacking Tyr-397, in a context

FAK without autophosphorylation

where its functionally related proteins and partners are expressed at levels close to normal.

Dramatic alteration of the phosphorylation response to cell adhesion in FAK^{ΔΔ} MEFs- We tested the effects of integrin engagement on the phosphorylation of FAK tyrosine residues in FAK^{ΔΔ} MEFs. As expected, plating wild-type MEFs on fibronectin (FN) induced the phosphorylation of wild type FAK on Tyr-397, Tyr-576/577, which allows its full enzymatic activation, and on Tyr-925, which regulates the recruitment of partners and downstream signaling pathways, as well as FAK localization to focal adhesions (16, 30) (Fig. 3A and Fig. 3B). In contrast, the FN-induced phosphorylation of these residues was lost in FAK^{ΔΔ} MEFs (Fig. 3A and Fig. 3B), although SFKs were similarly activated in wild type and mutant MEFs (data not shown). These results show that autophosphorylation on Tyr-397 is critical for SFK-dependent tyrosine phosphorylation of FAK and confirm that the moderate increase of FAK Δ basal kinase activity (Supplemental Fig. 2) has no effect on FAK activation and Src-mediated signaling. We also examined p130Cas and paxillin, whose phosphorylation by the FAK-SFK complex is important for cytoskeleton rearrangement and activation of downstream signaling pathways (17). The phosphorylation of both proteins was stimulated by FN in FAK^{+/+} but not in FAK^{ΔΔ} MEFs (Fig. 3C, D) despite a similar interaction of endogenous FAK and FAK Δ with both p130Cas and paxillin in these cells or after overexpression in COS7 (data not shown). In contrast, the phosphorylation of cortactin, which is known to be catalyzed by SFKs independently of FAK (27), was unaffected in FAK^{ΔΔ} cells (Fig. 3E). Previous studies proposed that the phosphorylation of p130Cas and paxillin by Src may be achieved through both FAK-dependent and independent mechanisms (29, 31). However, the absence of any significant phosphorylation of p130Cas and paxillin in FAK^{ΔΔ} cells plated on fibronectin suggests that FAK autophosphorylation is required for targeting SFKs to p130Cas and paxillin in response to integrin engagement.

Spreading and morphology are altered in FAK^{ΔΔ} fibroblasts and endothelial cells- Integrin engagement mediates the adhesion of many cell types and induces organized actin polymerization resulting in the extension of the membrane (lamellipodia) at the periphery of spreading cells. Since FAK plays a critical role in adhesion and spreading (4, 10, 28), we investigated the

consequences of exon 15 deletion on these processes. After 30 min on polylysine (PL) or FN, FAK^{ΔΔ} cells showed delayed spreading compared to FAK^{+/+} MEFs and lacked continuous smooth-round peripheral membrane extensions, characteristic of lamellipodia (Fig. 4A). Instead, FAK^{ΔΔ} cells exhibited multiple thinner membrane protrusions containing dense actin fibers (Fig. 4A). These narrow actin-rich membrane extensions of FAK^{ΔΔ} MEFs remained prominent after 1 hour on FN and were identified as abnormal lamellipodia since cortactin, which normally localizes at the edges of protruding lamellipodia, was localized at their tips (Fig. 4B). A similar phenotype was reported in several cell types lacking FAK expression (10, 32, 33). Lamellipodia formation and cell spreading in response to integrin engagement has been reported to require the release by FAK of the Arp2/3 complex bound to its FERM domain, triggered by autophosphorylation of Tyr-397 (32). Thus, the defects observed in FAK^{ΔΔ} cells may be due to the disruption of this mechanism. After 2 hours on FN, immunostaining of both cell types for vinculin, a protein localized at focal adhesions, showed an increase in the number and size of focal adhesions in FAK^{ΔΔ} MEFs compared to wild type cells (Fig. 4C). Both FAK^{+/+} and FAK^{ΔΔ} MEFs acquired an apparent typical fibroblastic stellate morphology with radial actin stress fibers after 20 hours on PL or FN (Fig. 4D). However, FAK^{ΔΔ} MEFs lacked the large lamellipodia observed in wild type. Furthermore, they displayed a persistent increase in the number and size of focal adhesions localized at the tips of stress fibers, characterized by a stronger enrichment of FAK immunoreactivity than in FAK^{+/+} MEFs (Fig. 4D). Since FAK^{ΔΔ} embryos showed important vascularization defects, we also monitored the properties of primary FAK^{ΔΔ} endothelial cells (EC) in response to integrin engagement. After 2 hours on FN, abnormal lamellipodia and cell spreading defects were observed in mutant EC which showed enlarged focal adhesions enriched in FAK Δ (Fig. 4E and F). Interestingly, a similar phenotype was reported in primary FAK^{-/-} EC (10), which also showed no increased expression of Pyk2. The enrichment of FAK Δ compared to FAK at focal adhesions, was also observed following its expression by transfection in FAK^{-/-} fibroblasts (data not shown) similarly to the mutant FAKY397F overexpressed in FAK^{-/-} cells (29). Since the phosphorylation of Tyr-925 is important

for the release of FAK from focal adhesions and their turnover (30), the deficit in FAK Tyr-925 phosphorylation that we observed in *FAK^{ΔΔ}* cells (Fig. 3A and B) may contribute to the increased number and size, of focal adhesions, and their enrichment in FAKΔ protein (Fig. 4A-F). The stellate morphology of *FAK^{ΔΔ}* MEFs contrasts with the ultraspread morphology of *FAK^{-/-}* fibroblasts stably expressing FAKY397F in the same experimental conditions (29). The high expression of Pyk2 and FAKY397F in these cells may be responsible for their different phenotype compared to *FAK^{ΔΔ}* MEFs that contain close to normal levels of Pyk2 and FAKΔ. Our results also demonstrate that *FAK^{ΔΔ}* cells have a delayed spreading characterized by disorganized lamellipodia, which never reach the same extent as in *FAK^{+/+}* MEFs, and an increased number and size of focal adhesions, enriched in FAKΔ. These defects, also observed in the mutant endothelial cells, may underlie the vascular abnormalities observed in *FAK^{ΔΔ}* embryos.

Proliferation of FAK^{ΔΔ} fibroblasts is decreased- FAK is implicated in the control of cell growth (28, 34), although its importance depends on cell types (19, 20, 35). We compared the proliferation of *FAK^{+/+}* and *FAK^{ΔΔ}* MEFs in standard culture conditions (10 % serum). No differences in proliferation between wild type and mutant MEFs were observed during the first 3 days. Thereafter, *FAK^{ΔΔ}* MEFs proliferated more slowly than *FAK^{+/+}* and they reached a lower saturation density (Fig. 5A). These results demonstrate that FAK autophosphorylation on Tyr-397 is required for normal proliferation of MEFs (Fig. 5A). However, growth of *FAK^{ΔΔ}* MEFs was mostly restored at a higher serum concentration (Fig. 5B), suggesting that the proliferative defect due to the lack of FAK autophosphorylation could be compensated by increased proliferative signals. *FAK^{-/-}* embryonic mesodermal cells *in vivo* or *FAK^{-/-}* fibroblasts *in vitro* also exhibited a proliferative defect attributed to an up-regulation of p53 (20, 36). This up-regulation may account for the use of a p53^{-/-} background to establish *FAK^{-/-}* fibroblasts (4). Indeed FAK FERM domain binds to and causes the degradation of p53, independently of its autophosphorylation and kinase activity (20, 37). However we showed that p53 was not increased in

FAK^{ΔΔ} MEFs (Fig. 2C). Thus, the lack of FAK autophosphorylation is likely to inhibit cell proliferation by an alternative pathway.

The contrast between the phenotype of *FAK^{-/-}* and *FAK^{ΔΔ}* embryos provides strong evidence for autophosphorylation-independent functions of FAK *in vivo*. Such functions have been suggested in cultured cells, in addition to the aforementioned regulation of p53 expression. For example, pharmacological inhibition of FAK did not block proliferation of tumor cells and did not block their apoptosis *in vitro* (19). Durotaxis, the ability of cells, cultured on a substrate of graded stiffness, to move from softer to stiffer regions, was abolished in *FAK^{-/-}* cells and rescued by FAKY397F, which did not rescue the migration speed (38). Furthermore, abnormal axonal branching in hippocampal *FAK^{-/-}* neurons was partially rescued by the expression of FAKY397F (7). Although very few *bona fide* substrates of FAK have been characterized in intact cells (1), the respective role of FAK catalytic activity and scaffolding properties will have to be determined in these autophosphorylation-independent functions. Auto-phosphorylation-independent function of FAK is also supported by the observation that although Tyr-397 is highly conserved in most metazoans, it is not found in *C. elegans* (21).

In conclusion, the study of *FAK^{ΔΔ}* mice provides important information about the role of FAK autophosphorylation on Tyr-397 *in vivo*. FAK autophosphorylation is not required for development before E13.5 but becomes necessary past that stage. The autophosphorylation of FAK on Tyr-397 is not necessary for general cell morphology in standard culture conditions or to repress p53 and Pyk2 expression. In contrast, it plays an important role in focal adhesion turnover, lamellipodia formation, cell spreading and proliferation. Thus, our results demonstrate that the physiological functions of FAK *in vivo* are achieved through both autophosphorylation-independent and autophosphorylation-dependent mechanisms and that the requirements for these mechanisms vary during development. They underline that identification of the mechanisms by which FAK regulates different cellular functions will be important to improve the design of appropriate therapeutic tools.

REFERENCES

1. Schlaepfer, D. D., Mitra, S. K., and Ilic, D. (2004) *Biochim Biophys Acta* **1692**, 77-102
2. Chatzizacharias, N. A., Kouraklis, G. P., and Theocharis, S. E. (2008) *Histol Histopathol* **23**, 629-650
3. Parsons, J. T. (2003) *J Cell Sci* **116**, 1409-1416
4. Ilic, D., Furuta, Y., Kanazawa, S., Takeda, N., Sobue, K., Nakatsuji, N., Nomura, S., Fujimoto, J., Okada, M., and Yamamoto, T. (1995) *Nature* **377**, 539-544
5. Shen, T. L., Park, A. Y., Alcaraz, A., Peng, X., Jang, I., Koni, P., Flavell, R. A., Gu, H., and Guan, J. L. (2005) *J Cell Biol* **169**, 941-952
6. Beggs, H. E., Schahin-Reed, D., Zang, K., Goebbels, S., Nave, K. A., Gorski, J., Jones, K. R., Sretavan, D., and Reichardt, L. F. (2003) *Neuron* **40**, 501-514
7. Rico, B., Beggs, H. E., Schahin-Reed, D., Kimes, N., Schmidt, A., and Reichardt, L. F. (2004) *Nat Neurosci* **7**, 1059-1069
8. Grove, M., Komiyama, N. H., Nave, K. A., Grant, S. G., Sherman, D. L., and Brophy, P. J. (2007) *J Cell Biol* **176**, 277-282
9. Nikolopoulos, S. N., and Giancotti, F. G. (2005) *Cell Cycle* **4**, e131-135
10. Braren, R., Hu, H., Kim, Y. H., Beggs, H. E., Reichardt, L. F., and Wang, R. (2006) *J Cell Biol* **172**, 151-162
11. Weis, S. M., Lim, S. T., Lutu-Fuga, K. M., Barnes, L. A., Chen, X. L., Gothert, J. R., Shen, T. L., Guan, J. L., Schlaepfer, D. D., and Cheresch, D. A. (2008) *J Cell Biol* **181**, 43-50
12. Vadali, K., Cai, X., and Schaller, M. D. (2007) *IUBMB Life* **59**, 709-716
13. Peng, X., Wu, X., Druso, J. E., Wei, H., Park, A. Y., Kraus, M. S., Alcaraz, A., Chen, J., Chien, S., Cerione, R. A., and Guan, J. L. (2008) *Proc Natl Acad Sci U S A* **105**, 6638-6643
14. Hakim, Z. S., Dimichele, L. A., Doherty, J. T., Homeister, J. W., Beggs, H. E., Reichardt, L. F., Schwartz, R. J., Brackhan, J., Smithies, O., Mack, C. P., and Taylor, J. M. (2007) *Mol Cell Biol* **27**, 5352-5364
15. Vallejo-Illarramendi, A., Zang, K., and Reichardt, L. F. (2009) *J Clin Invest* **119**, 2218-2230
16. Mitra, S. K., Hanson, D. A., and Schlaepfer, D. D. (2005) *Nat Rev Mol Cell Biol* **6**, 56-68
17. Hanks, S. K., Ryzhova, L., Shin, N. Y., and Brabek, J. (2003) *Front Biosci* **8**, d982-996
18. Playford, M. P., and Schaller, M. D. (2004) *Oncogene* **23**, 7928-7946
19. Slack-Davis, J. K., Martin, K. H., Tilghman, R. W., Iwanicki, M., Ung, E. J., Autry, C., Luzzio, M. J., Cooper, B., Kath, J. C., Roberts, W. G., and Parsons, J. T. (2007) *J Biol Chem* **282**, 14845-14852
20. Lim, S. T., Chen, X. L., Lim, Y., Hanson, D. A., Vo, T. T., Howerton, K., Larocque, N., Fisher, S. J., Schlaepfer, D. D., and Ilic, D. (2008) *Mol Cell* **29**, 9-22
21. Corsi, J. M., Rouer, E., Girault, J. A., and Enslin, H. (2006) *BMC Genomics* **7**, 198
22. Burgaya, F., Toutant, M., Studler, J. M., Costa, A., Le Bert, M., Gelman, M., and Girault, J. A. (1997) *J Biol Chem* **272**, 28720-28725
23. Toutant, M., Costa, A., Studler, J. M., Kadare, G., Carnaud, M., and Girault, J. A. (2002) *Mol Cell Biol* **22**, 7731-7743
24. Tournier, C., Hess, P., Yang, D. D., Xu, J., Turner, T. K., Nimmual, A., Bar-Sagi, D., Jones, S. N., Flavell, R. A., and Davis, R. J. (2000) *Science* **288**, 870-874
25. Sieg, D. J., Ilic, D., Jones, K. C., Damsky, C. H., Hunter, T., and Schlaepfer, D. D. (1998) *Embo J* **17**, 5933-5947
26. Furuta, Y., Ilic, D., Kanazawa, S., Takeda, N., Yamamoto, T., and Aizawa, S. (1995) *Oncogene* **11**, 1989-1995
27. Weed, S. A., and Parsons, J. T. (2001) *Oncogene* **20**, 6418-6434
28. Lim, Y., Lim, S. T., Tomar, A., Gardel, M., Bernard-Trifilo, J. A., Chen, X. L., Uryu, S. A., Canete-Soler, R., Zhai, J., Lin, H., Schlaepfer, W. W., Nalbant, P., Bokoch, G., Ilic, D., Waterman-Storer, C., and Schlaepfer, D. D. (2008) *J Cell Biol* **180**, 187-203
29. Owen, J. D., Ruest, P. J., Fry, D. W., and Hanks, S. K. (1999) *Mol Cell Biol* **19**, 4806-4818
30. Katz, B. Z., Romer, L., Miyamoto, S., Volberg, T., Matsumoto, K., Cukierman, E., Geiger, B., and Yamada, K. M. (2003) *J Biol Chem* **278**, 29115-29120
31. Ruest, P. J., Shin, N. Y., Polte, T. R., Zhang, X., and Hanks, S. K. (2001) *Mol Cell Biol* **21**, 7641-7652
32. Serrels, B., Serrels, A., Brunton, V. G., Holt, M., McLean, G. W., Gray, C. H., Jones, G. E., and Frame, M. C. (2007) *Nat Cell Biol* **9**, 1046-1056
33. Tilghman, R. W., Slack-Davis, J. K., Sergina, N., Martin, K. H., Iwanicki, M., Hershey, E. D., Beggs, H. E., Reichardt, L. F., and Parsons, J. T. (2005) *J Cell Sci* **118**, 2613-2623
34. Cox, B. D., Natarajan, M., Stettner, M. R., and Gladson, C. L. (2006) *J Cell Biochem* **99**, 35-52
35. Schober, M., Raghavan, S., Nikolova, M., Polak, L., Pasolli, H. A., Beggs, H. E., Reichardt, L. F., and Fuchs, E. (2007) *J Cell Biol* **176**, 667-680

FAK without autophosphorylation

36. Cance, W. G., and Golubovskaya, V. M. (2008) *Sci Signal* **1**, pe22
37. Golubovskaya, V. M., Finch, R., and Cance, W. G. (2005) *J Biol Chem* **280**, 25008-25021
38. Wang, H. B., Dembo, M., Hanks, S. K., and Wang, Y. (2001) *Proc Natl Acad Sci U S A* **98**, 11295-11300

ACKNOWLEDGEMENTS

The authors thank D. Ilic (StemLifeline Inc) for providing *FAK^{-/-}* MEF, S. Marullo and C. Boularan (Institut Cochin, Inserm U567) for providing the Luc-p53 plasmid, I. Bachy (Karolinska Institutet, Stockholm Sweden), M. Holzenberger (Inserm UMR-S893), P. Gaspar, D. Hervé, J. Bertran-Gonzalez, R-M. Mège (Inserm UMR-S U839) and J. Chelly (Institut Cochin, Inserm UMR-S567), for helpful discussions as well as members of the “Plateforme de Recombinaison Homologue” (Institut Cochin, Inserm UMR-S567, CNRS UMR8104), of the Cell Imaging and Animal Facilities and S. Clain (Inserm UMR-S839) for their help. This work was supported by Inserm and by grants from the *Association pour la Recherche sur le Cancer* to H.E. (3746) and to J.A.G. (3138), and from *Agence Nationale de la Recherche* (ANR-05-2_42589) to J.A.G.

FIGURE LEGENDS

Figure 1: Late defects and lethality in *FAK^{ΔΔ}* embryos. (A) Schematic FAK and FAK Δ structure, showing the N-terminal FERM domain, the kinase domain and the C-terminal focal adhesion targeting (FAT) domain, as well as proline-rich sequences (PR1-3). FAK Δ lacks 19 amino acids in the FERM-kinase linker, including Tyr-397. (B) Comparison of the *in utero* survival curves of FAK-null and FAK $\Delta\Delta$ embryos (red inverted triangles). The data concerning FAK-null embryos are from (26) (FAK $^{-/-}$, green squares) and (5) (CFKO, magenta triangles). (C) Appearance of FAK $^{+/+}$ and FAK $\Delta\Delta$ embryos at E13.5 and E15.5 (arrows: hemorrhages; arrowheads: edemas). Gross morphology defects of E14.5 FAK $^{+/+}$ and FAK $\Delta\Delta$ lungs, heart, and liver (scale bars, 1 mm). E14.5 (upper panel) and E15.5 (lower panel) anterior (left) and posterior (right) footplates (scale bars, 1 mm). (D) FAK $\Delta\Delta$ embryos show delayed artery formation and vascular remodeling defects. Whole-mount triple immunofluorescence confocal microscopy using antibodies to SMA (Smooth Muscle Actin, green), PECAM1 (red) and neurons (TUJ1) (blue) on skin from E14.5 embryos. Confocal microscopy images were acquired using 10X magnification.

Figure 2: Expression of FAK-associated proteins in tissue from FAK $\Delta\Delta$ embryos and mutant MEFs. (A) Immunoblotting of phospho-Tyr-397 (pY397), FAK, vinculin (Vinc), p130-Cas (Cas), paxillin (Pax), cortactin (Cort), Src and Fyn in liver lysates from FAK $^{+/+}$, FAK $^{+/\Delta}$ and FAK $\Delta\Delta$ E14.5 littermate embryos. (B) Immunoblotting of the same proteins as in (A), Pyk2, and GAPDH in MEFs derived from E12.5 FAK $^{+/+}$ and FAK $\Delta\Delta$ littermate embryos. (C) Immunoblotting for p53 in MEFs as in (B), Lysates from COS7 cells expressing a fusion luciferase-p53 protein was used as a control for p53 immunoreactivity.

Figure 3: Alteration of the phosphorylation response to integrin engagement in FAK $\Delta\Delta$ MEFs. MEFs were plated on polylysine (Pl) or fibronectin (Fn) for 30 min before lysis and immunoblottings for phospho-Tyr-397, 576, 577, 925 and total FAK (A) and quantified (B). Immunoblotting of tyrosine phosphorylated (p, upper panels) and total levels (middle panels) of Cas (C), Pax (D), and Cort (E) in MEFs plated as in (A). These experiments have been repeated with independent FAK $^{+/+}$ or FAK $\Delta\Delta$ (n=3 for each genotype) MEFs populations established from different littermate embryos. Quantified data (means \pm SEM n= 3) were analyzed using two-way ANOVA. Bonferroni post-test: * $p < 0.05$, ** $p < 0.01$, *** $p < 0.001$.

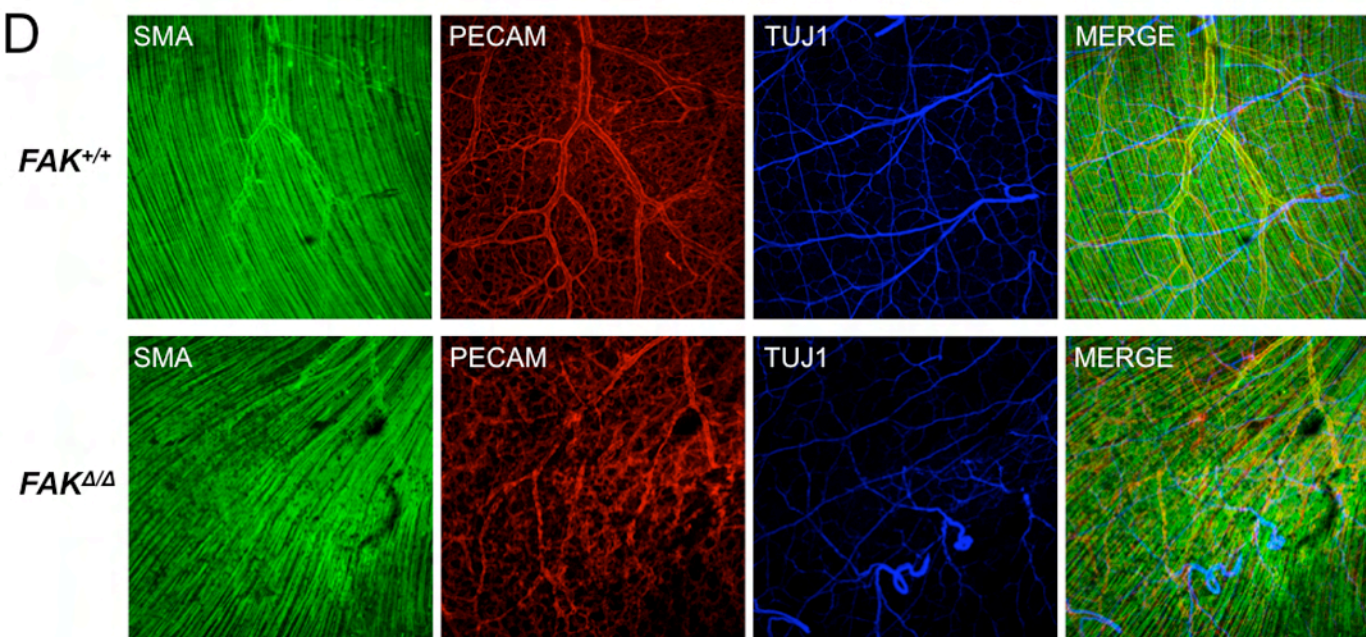
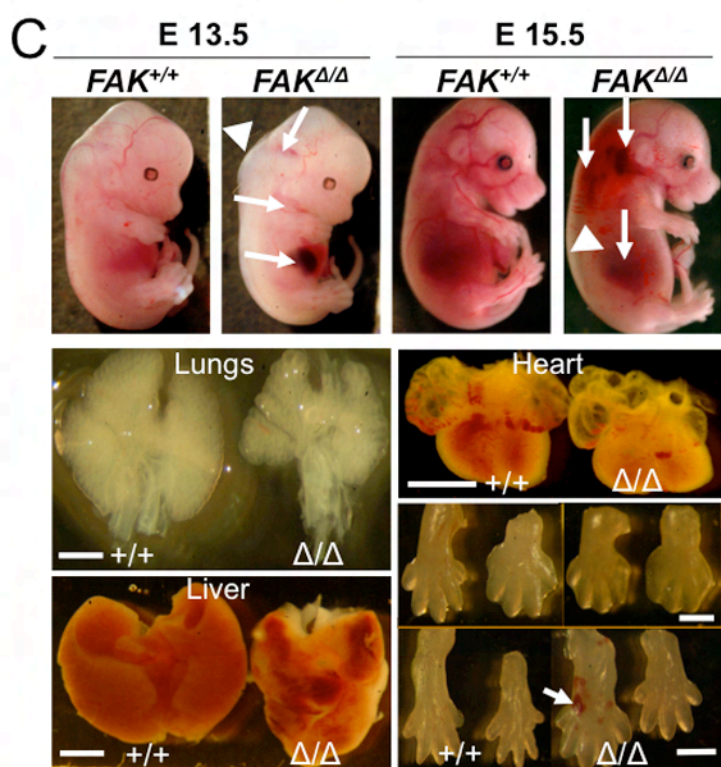
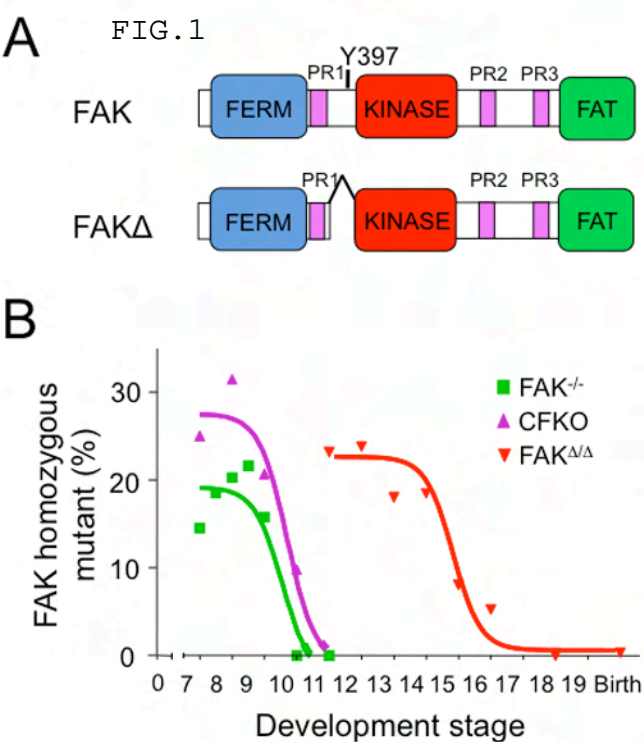
Figure 4: Delayed spreading and abnormal lamellipodia in FAK $\Delta\Delta$ fibroblasts and endothelial cells. FAK $^{+/+}$ and FAK $\Delta\Delta$ MEFs or endothelial cells (EC) were plated on polylysine (Pl) or fibronectin (Fn) for 0.5-20 h as indicated. Cells were stained for actin with rhodamin-conjugated phalloidin (A-D, F) and/or antibodies recognizing FAK (A, D, E), cortactin (B, F), vinculin (C, F) and revealed with FITC-conjugated secondary antibody. EC cells (E, F) were identified by CD31 immunostaining. Lamellipodia were well developed in wild type (arrows) but not mutant cells (A-B and D-F), which displayed narrow cortactin-positive protrusions (B, F). Focal adhesions were more numerous and larger in FAK $\Delta\Delta$ than wild type cells (C, D, E, F). Scale bars: 20 μ m.

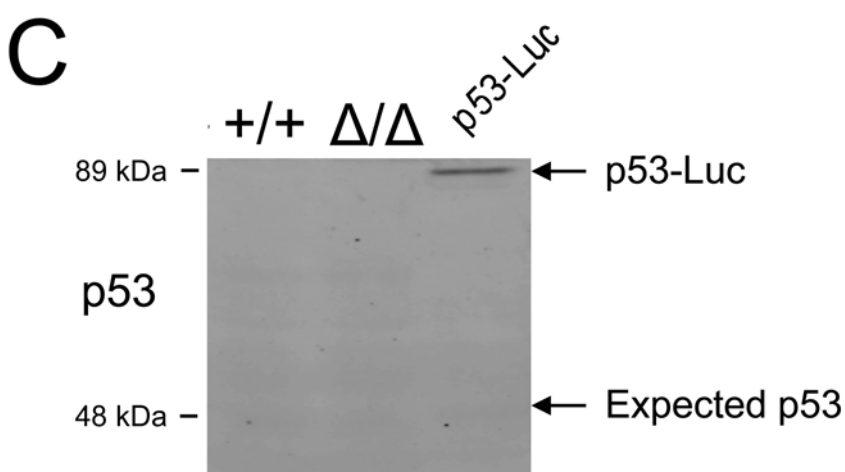
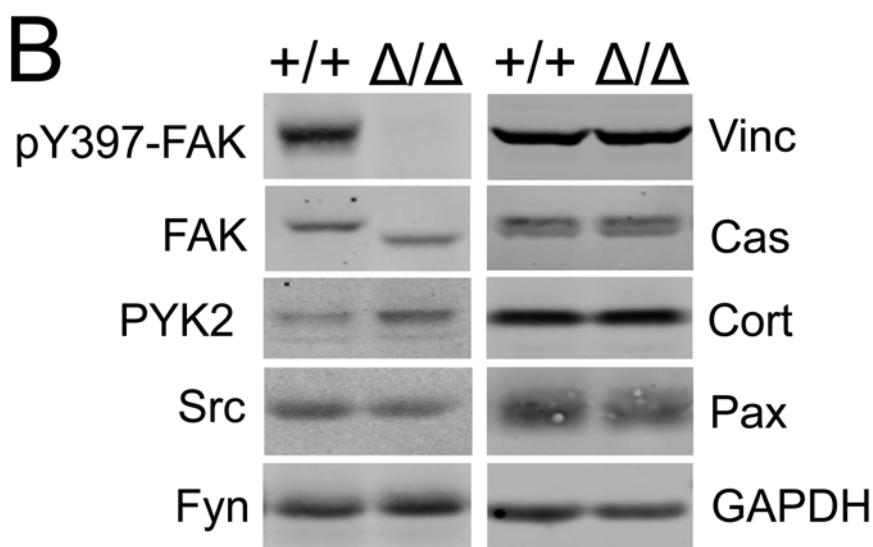
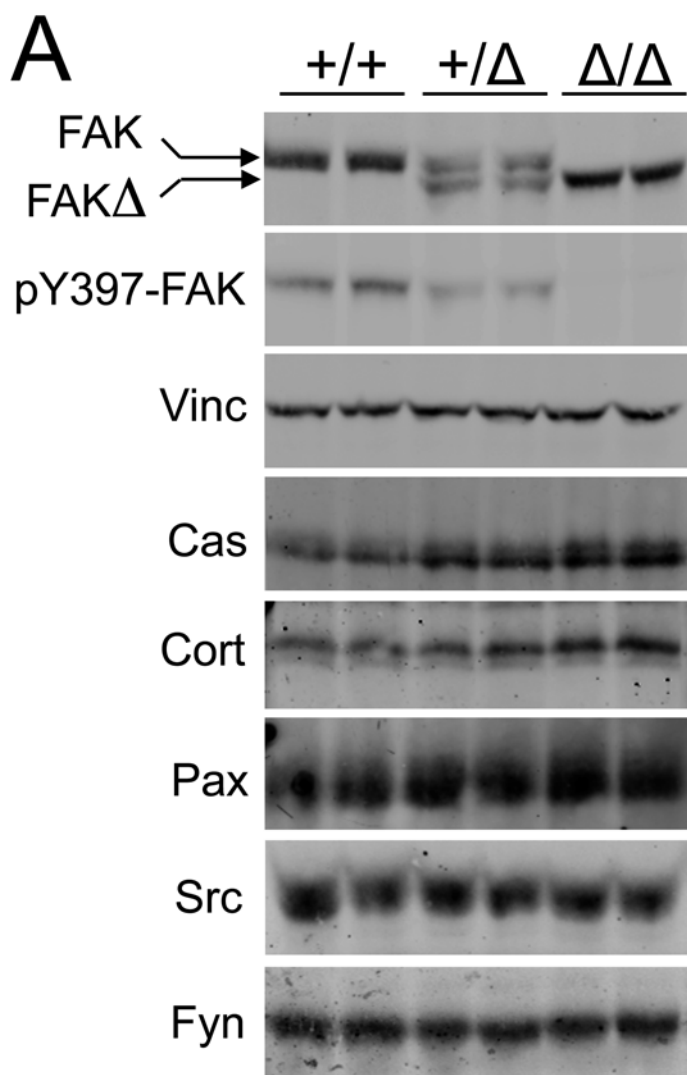
Figure 5: Proliferation is slowed in FAK $\Delta\Delta$ MEFs. (A) Independent MEFs populations (n=3-4 for each genotype) established from littermate embryos were plated separately in triplicate (7500 cells/well) and grown in 10% serum, for the indicated number of days. Cell number was evaluated by crystal violet staining and the day after plating was considered as D=0. (B) FAK $^{+/+}$ and FAK $\Delta\Delta$ MEFs populations were grown in the indicated serum concentrations and counted by crystal violet staining at D=0 or after 7 days in culture (D=7). Data (means \pm SEM n= 3-4) were analyzed using two-way ANOVA. Bonferroni post-test: ** $p < 0.01$, *** $p < 0.001$.

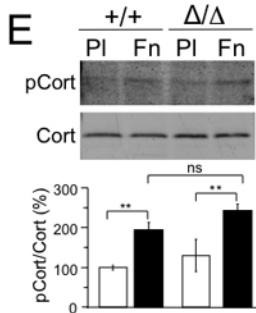
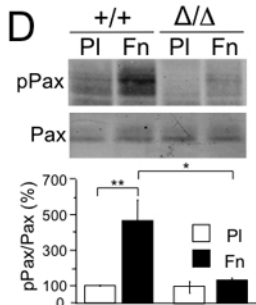
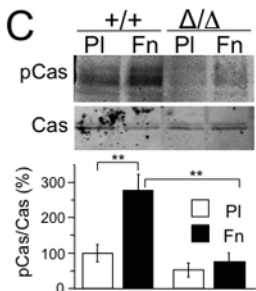
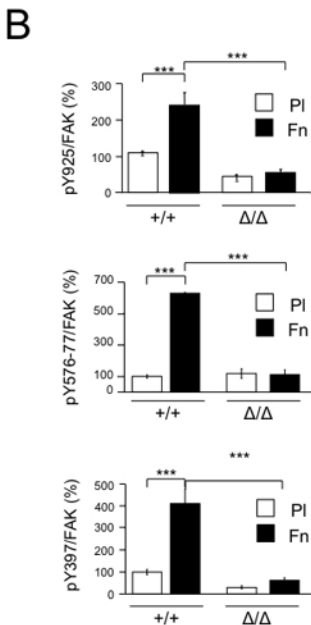
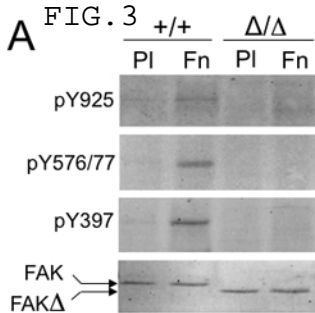
FAK without autophosphorylation

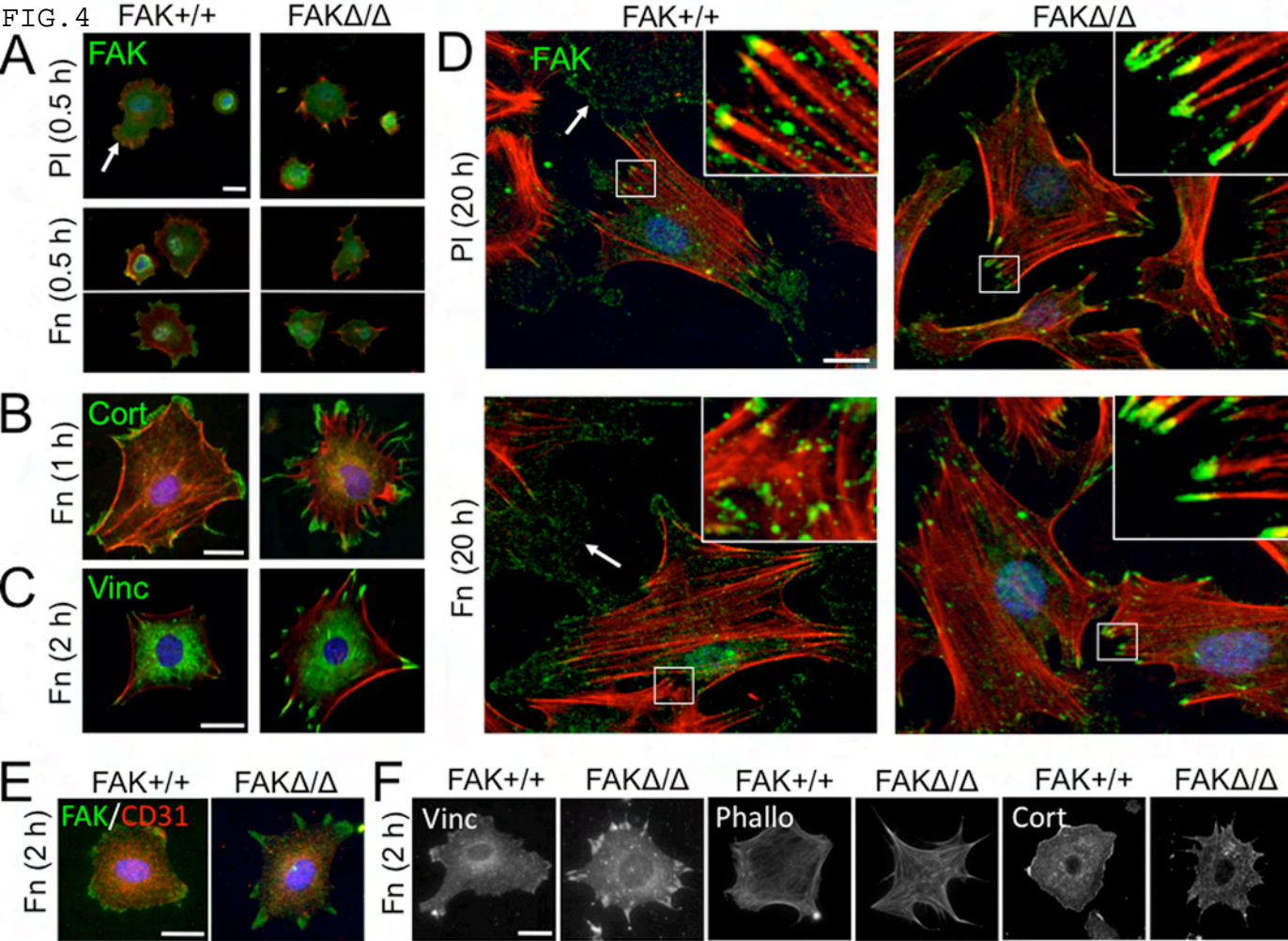
Table 1: Genotype of embryos obtained from crosses between $FAK^{+/Δ}$ mice. The total number of embryos (alive or dead) of each genotype obtained from crosses between ($FAK^{+/Δ}$) mice is indicated at various embryonic ages and birth. The number of dead embryos is indicated between parentheses.

Embryonic day	11.5	12.5	13.5	14.5	15.5	16.5	18.5	Born
+/+	20 (1)	11(1)	22	30	18 (1)	16	10	213
+/ $Δ$	46 (2)	22	78	84 (5)	51 (1)	39 (1)	17	416
$Δ/Δ$	26 (7)	10	33 (11)	42 (17)	11 (5)	7 (4)	1 (1)	3
Number of litters	12	5	18	21	11	6	5	94

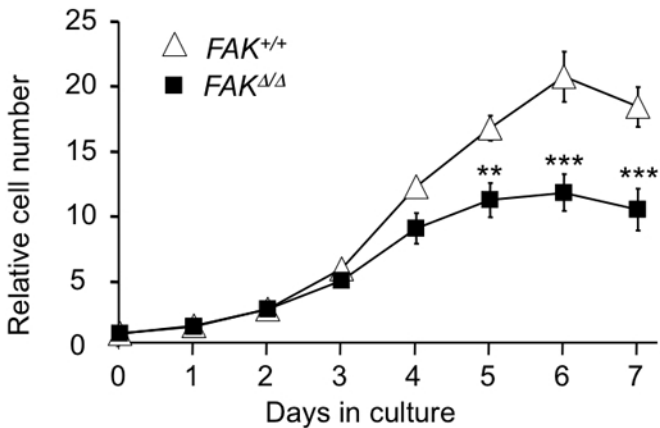




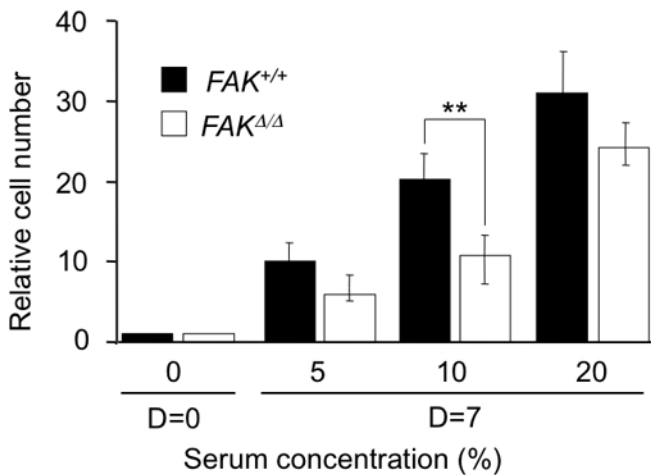




A



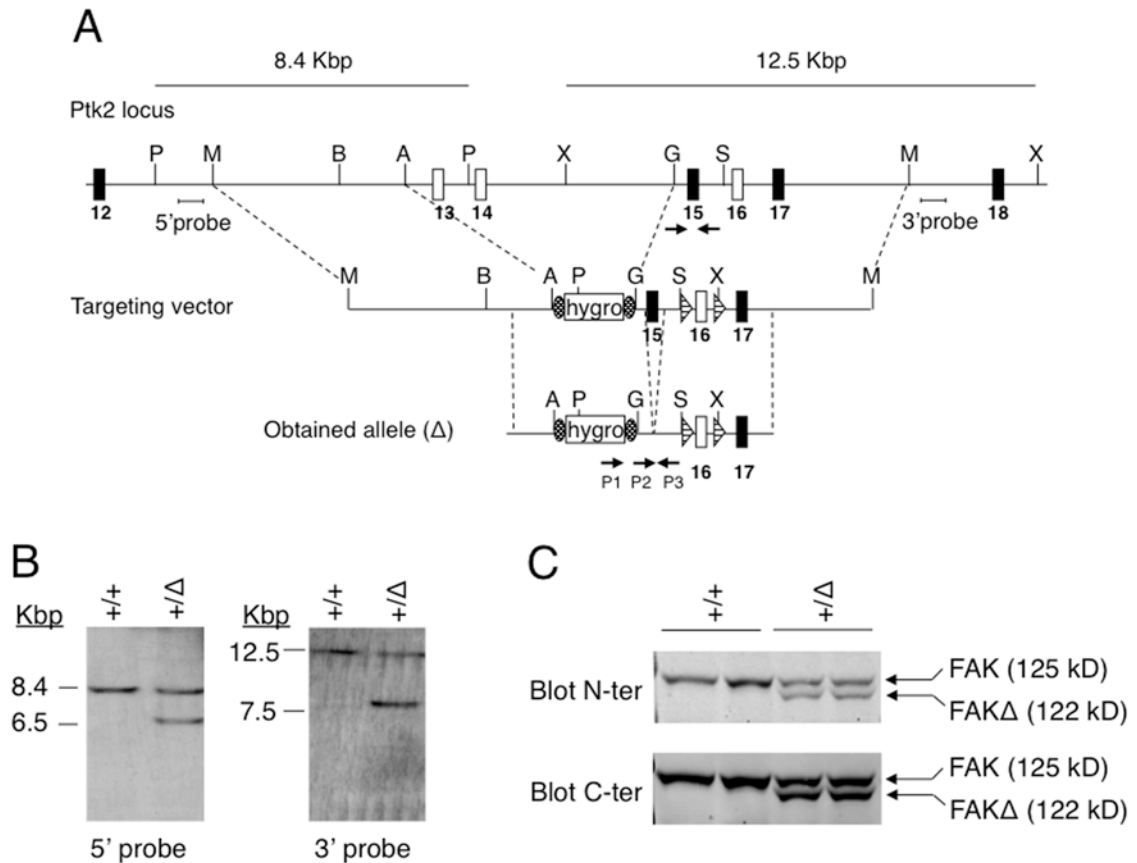
B



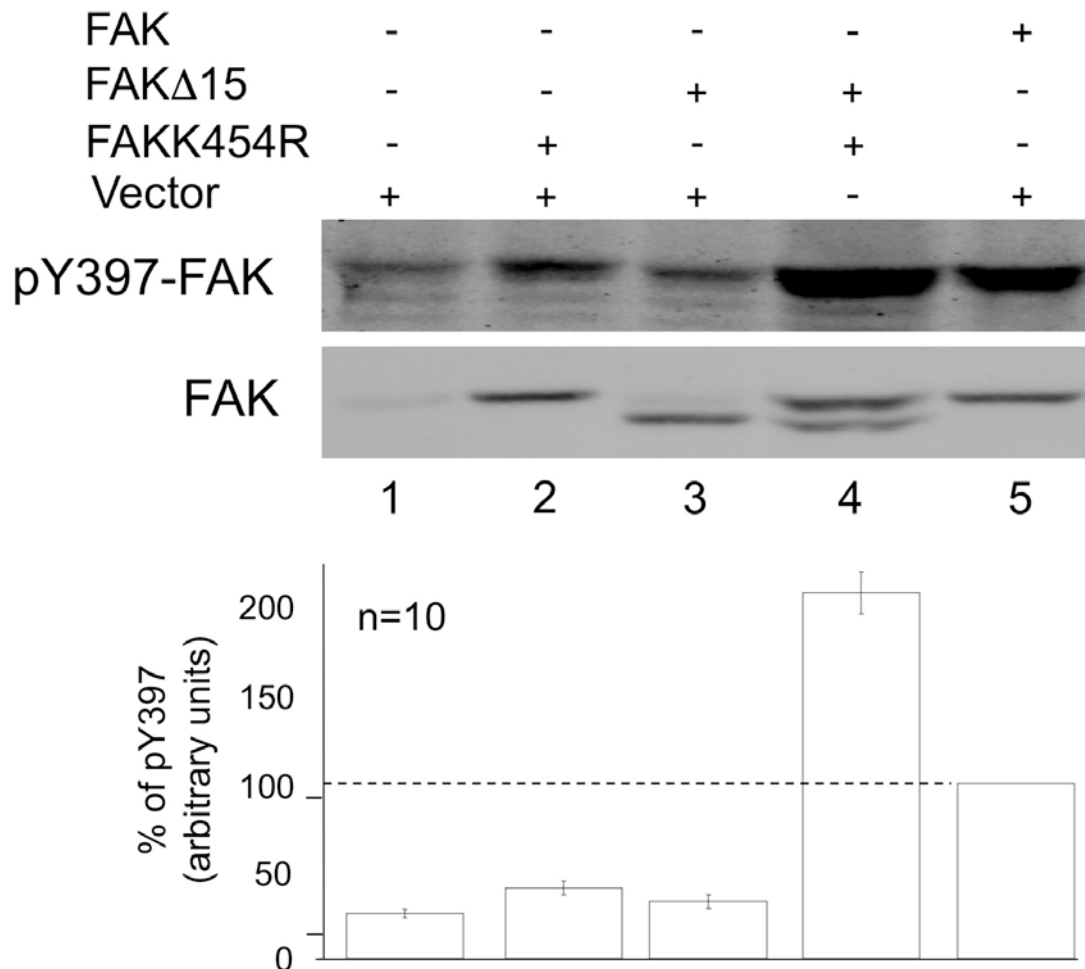
Supplemental Data for

Autophosphorylation-independent and dependent functions of Focal Adhesion Kinase during development

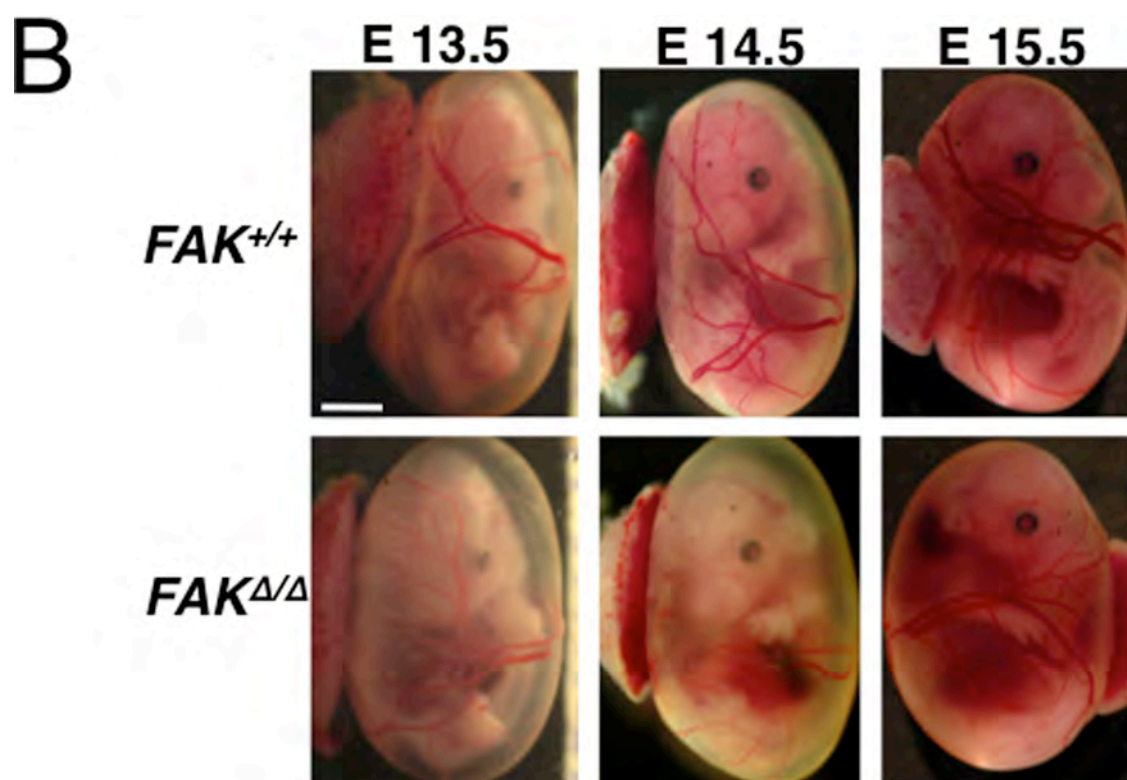
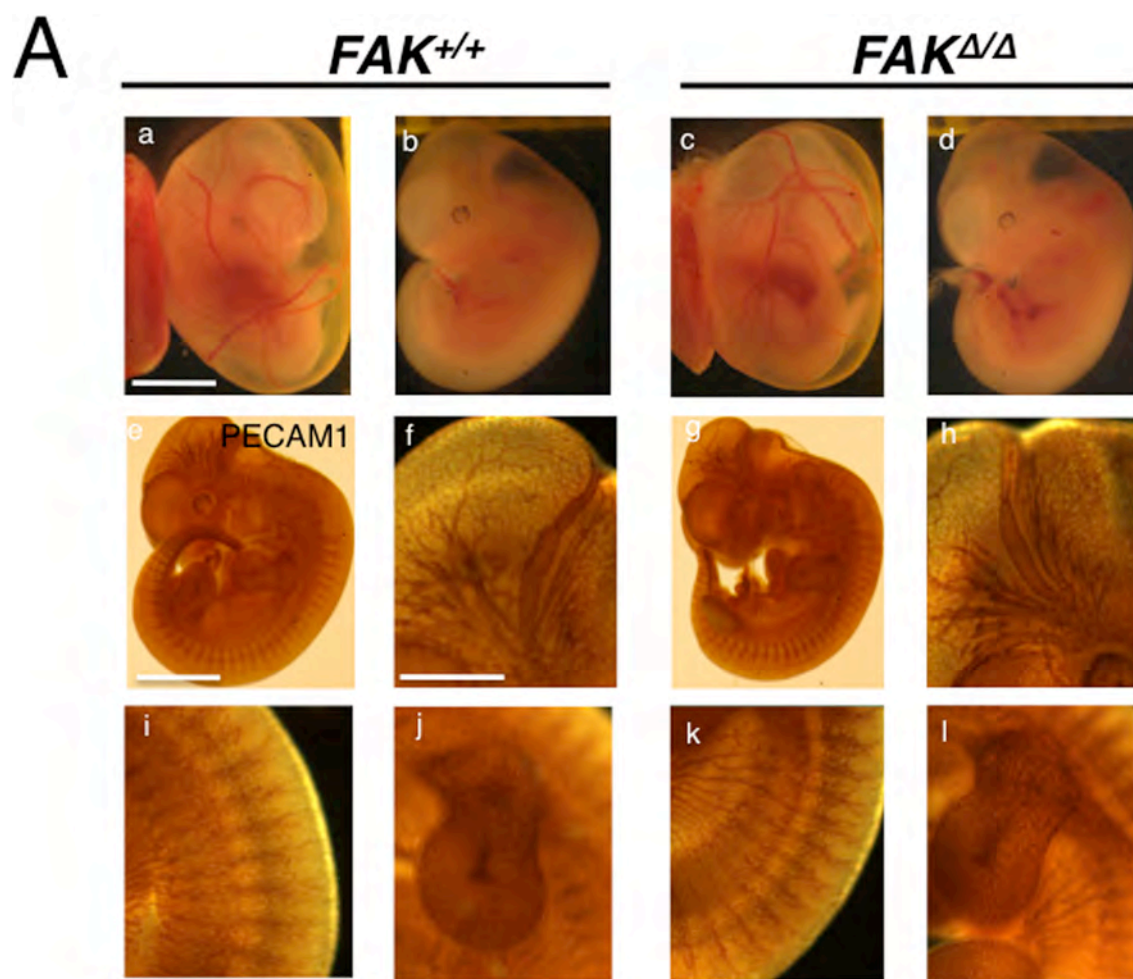
Jean-Marc Corsi, Christophe Houbron, Pierre Billuart, Isabelle Brunet, Karine Bouvrée, Anne Eichmann, Jean-Antoine Girault and Hervé Enslin



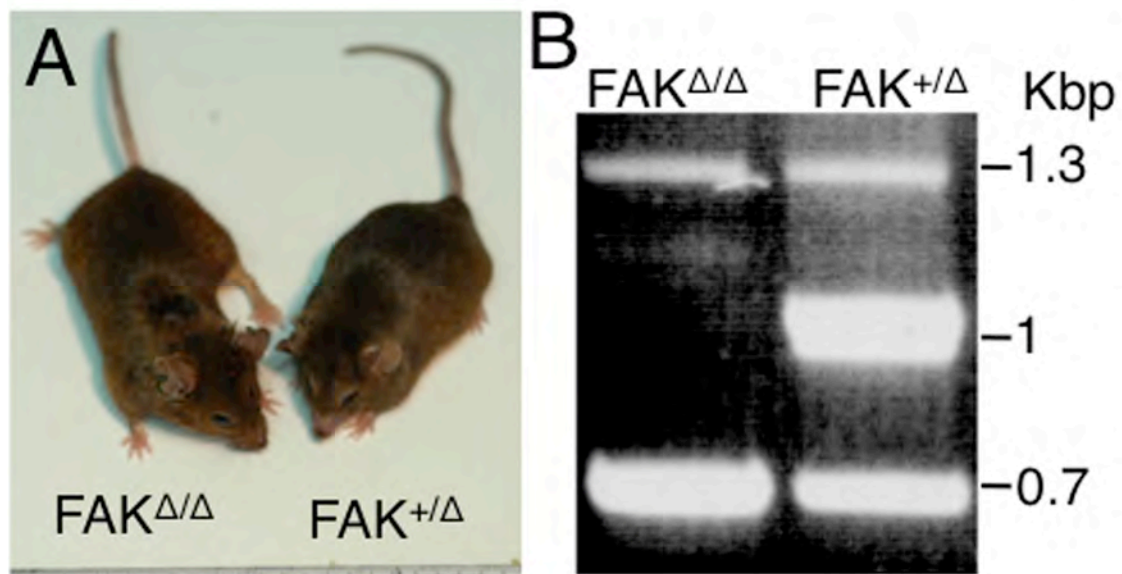
Suppl. Fig. 1: Generation and analysis of $FAK^{\Delta/\Delta}$ mutant mice. (A) Structure and restriction maps of the wild-type mouse FAK ($Ptk2$) gene, targeting vector and the obtained allele. Constitutive and alternative exons are figured by dark or white vertical boxes respectively, with their number (Corsi et al., 2006) indicated below. The insertion of a pgk-hygromycin (HYGRO)-resistance cassette flanked with FRT sites (ovals) allowed the deletion of alternative exons 13 and 14, and the positive selection of the homologous recombination event. Note that deletion of exons 13 and 14 is expected to have no consequence during early embryogenesis since they are not detected in mRNA during the first part of embryonic development [Corsi, 2006 #26]. The LoxP sequences (triangles) flanking the alternative exon 16 were placed for possible conditional deletion of this exon by the Cre recombinase. The position of the 5' and 3' probes used for Southern blots are indicated. Arrows represent the position of the primers (P1, P2, P3) used for genotyping by PCR. Abbreviations for the restriction sites are: P: *PstI*, M: *MstII*, B: *BamHI*, A: *BstI*, X: *XmnI*, G: *BglIII*, S: *SfiI*. (B) Southern blot analyses of the ES cells clones. ES clones were electroporated and cultured at the *Homologous recombination-transgenic core facility* of the Cochin Institute. Genomic DNA was digested with *PstI* (5') or *XmnI* (3'). The wild-type allele produced an 8.4 kb fragment with the 5' probe and a 12.5 kb with the 3' probe, while the targeted allele produced a 6.5 kb fragment with the 5' probe and a 7.5 kb fragment with the 3' probe. (C) Immunoblot analyses of FAK and FAK Δ expression in wild-type (+/+) and heterozygous (+/Δ) F1 adult mice. The results obtained from two mice of each genotype are shown. Immunoblotting of proteins extracted from liver or other organs (data not shown) was carried out with antibodies recognizing specifically the N-terminal (top panel, blot N-ter) or the C-terminal (bottom panel, blot C-ter) domain of FAK.



Suppl. Fig. 2: Transphosphorylation of FAK Tyr-397 in COS7 cells. To determine whether FAK Δ was active in cells we used the ability of FAK to undergo *trans* autophosphorylation in intact cells (ref Toutant et al, MCB 2002). COS7 cells were transfected with FAK, FAK Δ and FAKK454R, the kinase-dead form of FAK, alone or with a combination of FAK Δ and FAKK454R. Immunoblotting of cell lysates was carried out with antibodies recognizing specifically FAK phosphorylated on Tyr-397 or independently of its phosphorylation state. As expected wild-type FAK was phosphorylated on Tyr-397 (lane 5) whereas neither FAK-K454R (lane 2) nor FAK Δ (lane 3) transfected alone were phosphorylated compared to control cells (lane 1). In contrast when these two mutated forms of FAK were transfected together, phosphorylation of FAK-K454R on Tyr-397 was observed (lane 4). These results demonstrate that FAK Δ is an active kinase. Bar graphs represent the level of Tyr-397 autophosphorylation in each condition, expressed as a percentage \pm sem of autophosphorylation of transfected normal FAK (lane 5), set to 100% (n=10).



Suppl. Fig. 3: (A) *FAK^{ΔΔ}* embryos appear normal at E11.5. (a-d) Gross morphology of *FAK^{+/+}* (a, b) and *FAK^{ΔΔ}* (c, d) E11.5 embryos in the yolk sac (a, c) or outside of the yolk sac (b, d). (e-l) whole mount PECAM-1 immunohistochemistry of E11.5 embryos. Pictures of the whole embryos (e, g) and magnified pictures of the top of the head (f, h), the somites (i, k) and the forelimb (j, l) are shown. No vasculature abnormality was detected at that age. Embryos were examined and photographed on a dissecting microscope (model DMIL; Leica) with a progressive 3CCD camera (Cool Snap Photometrics, Roper Scientific) and QED capture version 2.0.33 (Media Cybernetics) at RT. (B) Vascular abnormalities in the yolk sac of *FAK^{ΔΔ}* embryos after E13.5. Pictures of *FAK^{+/+}* and *FAK^{ΔΔ}* embryos in their yolk sacs at E13.5, E14.5, and E15.5 are shown. Scale bars in A: a,e, 2mm; f, 1mm; in B: 2mm.



Suppl. Fig. 4: Rare $FAK^{\Delta/\Delta}$ mice survive to adulthood. (A) Heterozygous ($FAK^{+/\Delta}$) and homozygous ($FAK^{\Delta/\Delta}$) adult mice at 12 months. Three viable adult homozygous mice were obtained among a total of 632 genotyped mice from 94 litters. These mice crossed with wild type mice were fertile. (B) PCR analysis confirmed the genotype of adult mutant mice. Primers used were: P1: 5'-GTAGAAGTACTCGCCGATAG-3', P2: 5'-AATCACTCCAGTATAGTGCC-3' and P3: 5'-CCTTAGATGTGGGTCTTAAT-3' and their localization on the *fak* gene is shown in Supplemental figure 1A. The combination of the P1 and P3 primers selectively amplified a 1.3 kb fragment from the FAK^{Δ} allele. The combination of the P2 and P3 primers amplified a 0.7 kb fragment from the FAK^{Δ} allele and a 1 kb fragment from the wild type allele respectively. Fragments were separated on 0.8% agarose gels. The three products are seen in a heterozygous $FAK^{+/\Delta}$ mouse, whereas the band corresponding to the wild type allele is absent in an adult homozygous mutant mouse ($FAK^{\Delta/\Delta}$).